

Cite this: *Chem. Commun.*, 2011, **47**, 8799–8801

www.rsc.org/chemcomm

COMMUNICATION

Assembly of a family of mixed metal {Mo : V} polyoxometalates templated by TeO_3^{2-} : { $\text{Mo}_{12}\text{V}_{12}\text{Te}_3$ }, { $\text{Mo}_{12}\text{V}_{12}\text{Te}_2$ } and { $\text{Mo}_{17}\text{V}_8\text{Te}$ }[†]

M. Nieves Corella-Ochoa, Haralampos N. Miras, Alastair Kidd, De-Liang Long and Leroy Cronin*

Received 12th May 2011, Accepted 8th June 2011

DOI: 10.1039/c1cc12782a

The influence of the pyramidal heteroanion, TeO_3^{2-} in the self-assembly of mixed metal (Mo/V) systems, is demonstrated by the isolation of three novel mixed-metal, mixed-valence architectures, { $\text{Mo}_{12}\text{V}_{12}\text{Te}_3$ } (1), { $\text{Mo}_{12}\text{V}_{12}\text{Te}_2$ } (2) and { $\text{Mo}_{17}\text{V}_8\text{Te}$ } (3) with the tellurium centres exhibiting the novel μ_8 - TeO_4 and μ_9 - TeO_3 coordination modes while compounds 1 and 2 were discovered utilizing ESI mass spectrometry.

Polyoxometalate chemistry has undergone an exponential growth over the last few decades due to the vast range of properties and applications that this diverse family of inorganic materials presents.^{1,2} In this respect, there are numerous reported examples in the recent literature, where the architecture of new heteropolyoxometalates (HPOMs) is mainly templated by tetrahedral heteroanions, such as phosphates³ and sulfates.⁴ However, HPOMs templated by non-conventional (pyramidal⁵ or octahedral)⁶ heteroanions are relatively rare. Moreover, it has been demonstrated that the incorporation of pyramidal heteroanions with a non-bonding, but stereochemically active lone pair of electrons, influences the assembly process and consequently the observable structural features leading finally to unique archetypes with extraordinary properties.^{6a,7} In an effort to investigate the implication of the heteroanions mentioned above, we recently reported the characterization of two novel sulfite-based polyoxometalates with unprecedented mixed-metal/valence archetypes, [$\text{Mo}_{11}\text{V}_7\text{O}_{52}(\mu_9\text{-SO}_3)$]⁷⁻ (M_{18}S) and [$\text{Mo}_{11}\text{V}_7\text{O}_{52}(\mu_9\text{-SO}_3)(\text{Mo}_6\text{VO}_{22})$]¹⁰⁻ (M_{25}S), and we showed the use of reactive POM-based species as secondary building units towards the design of higher nuclearity architectures.^{8,9}

Herein, in order to investigate the effect of the geometry and the size of the incorporated heteroanions on the self-assembly process and the final structural motif, we report the synthesis, solid state and solution characterization of three novel tellurite-based mixed-metal and mixed-valence polyoxometalates, namely: $(\text{NH}_4)_9\text{K}[\text{Mo}_{12}^{\text{VI}}\text{V}_8^{\text{V}}\text{V}_4^{\text{IV}}\text{Te}^{\text{IV}}\text{O}_{69}(\mu_9\text{-Te}^{\text{IV}}\text{O}_3)_2]\cdot 27\text{H}_2\text{O}$ **1**,

$\text{K}_{14}[\text{Mo}_{12}^{\text{VI}}\text{V}_8^{\text{V}}\text{V}_4^{\text{IV}}\text{O}_{69}(\mu_9\text{-Te}^{\text{IV}}\text{O}_3)_2]\cdot 27\text{H}_2\text{O}$ **2**, which are isostructural with a tellurium centre gating the square shaped window on the cap of **1**; and $\text{K}_{10}[\text{Mo}_{11}^{\text{VI}}\text{V}_5^{\text{V}}\text{V}_2^{\text{IV}}\text{O}_{52}(\mu_9\text{-Te}^{\text{IV}}\text{O}_3)(\text{Mo}_6^{\text{VI}}\text{V}^{\text{VO}}\text{O}_{22})]\cdot 15\text{H}_2\text{O}$ **3**. To the best of our knowledge **1**, **2** and **3** are the largest tellurite-based mixed-metal polyoxometalate clusters reported to date, and it is the first time that the tellurite anion exhibits the μ_8 - and the rare μ_9 -coordination modes respectively. All three compounds were characterized in the solid state by X-ray structural analysis while compounds **1** and **2** were also characterized in solution by electrospray mass spectrometry studies.^{8,9} The sequential addition of NH_4VO_3 , $\text{K}_2\text{Te}^{\text{IV}}\text{O}_3$ and $\text{NH}_2\text{NH}_2\cdot 2\text{HCl}$ in an aqueous solution of $(\text{NH}_4)_6\text{Mo}^{\text{VI}}_7\text{O}_{24}$, followed by the adjustment of the pH by conc. HCl, resulted in the formation of dark green crystals of **1**;[‡] when KV^{VO}_3 and K_2MoO_4 were used instead of the ammonium salts, crystals of **2** were formed in similar yield.[‡] Even though sulphur and tellurium, belong to the same group of the periodic table and present similar behaviour under the same experimental conditions, the much larger size of the tellurium influenced the self-assembly process and the architecture of the final product (Fig. 1).

It is interesting to point out the chemical and structural information common to all three compounds: (a) the existence of the oxidized form of V in the presence of a reducing agent, even though the V^{V} is reduced rapidly to V^{IV} by the hydrazine (in the present case there are 4 V^{IV} for compounds **1** and **2**, and 2 for compound **3**); (b) the plethora of geometries adopted by the metal centres in the same structure, as shown by structural analysis (dioxo-/oxo- Mo^{VI} and octahedrally/ tetrahedrally coordinated $\text{V}^{\text{IV/V}}$ centres); and (c) the second reported

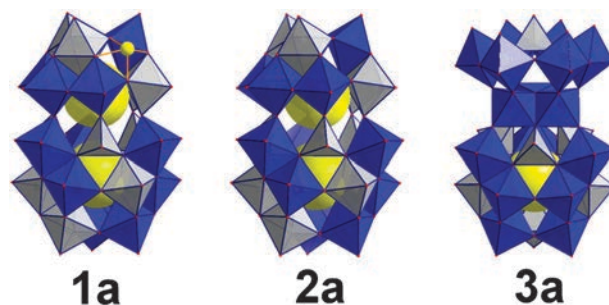


Fig. 1 Polyhedral representation of the three tellurite-based clusters. Colour code: Mo: blue polyhedra; V: grey polyhedra; Te: yellow spheres.

WestCHEM, Department of Chemistry, University of Glasgow, Glasgow G12 8QQ, Scotland, U.K. E-mail: L.Cronin@chem.gla.ac.uk; Web: <http://www.chem.gla.ac.uk/staff/lee>

[†] Electronic supplementary information (ESI) available: Syntheses, details and graphs describing UV-Vis, IR, TGA, redox titrations and ESI-MS for compound **1**, **2** and **3**. CCDC 825828–825830. For ESI and crystallographic data in CIF or other electronic format see DOI: 10.1039/c1cc12782a

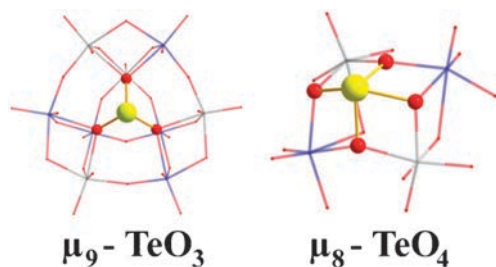


Fig. 2 Wire-stick representation of Te^{IV} coordination modes. $\mu_9\text{-TeO}_3$ (left) where each oxygen is linked to three metal centres, found in **1a** and **2a** upper and lower hemisphere and in **3a** lower hemisphere $\mu_8\text{-TeO}_4$ (right) in **1a** where every oxygen atom is bridged to two metal centres.

example of $\mu_9\text{-Te}^{\text{IV}}\text{O}_3$ coordination mode in the literature and the new $\mu_8\text{-Te}^{\text{IV}}\text{O}_4$ coordination mode in **1** (Fig. 2).

It is worth noting that the heteroanion size has a profound effect on the self-assembly of the metal oxide units in solution: the bigger the heteroanion becomes, the more spatial restrictions are introduced and this leads to new architectures with higher nuclearity as in the case of compounds **1** and **2**.

Crystallographic studies revealed that **1a** and **2a** can be formulated as $[\text{Mo}^{\text{VI}}_{12}\text{V}^{\text{V}}_8\text{V}^{\text{IV}}_4\text{Te}^{\text{IV}}\text{O}_{69}(\mu_9\text{-Te}^{\text{IV}}\text{O}_3)_2]^{10-}$ and $[\text{Mo}^{\text{VI}}_{12}\text{V}^{\text{V}}_8\text{V}^{\text{IV}}_4\text{O}_{69}(\mu_9\text{-Te}^{\text{IV}}\text{O}_3)_2]^{14-}$ respectively whereby the molybdovanadate-tellurite anions **1a** and **2a** adopt a “capsule” like structure which consists of two hemispheres. The upper hemisphere, which is structurally related to the lacunary Keggin structure $[\text{XM}_9\text{O}_{34}]^{n-}$,¹⁰ incorporates five V (3 V^{V} and 2 V^{IV}) and four Mo^{VI} centres crystallographically disordered over the nine positions. Its cavity is occupied by one $\mu_9\text{-Te}^{\text{IV}}\text{O}_3$ anion with the lone pair of electrons pointing downwards. In the case of **1a** a tellurite ion gates one of the square shaped windows of the M_9 cage (Fig. 2). The upper hemisphere is connected further to the lower half *via* the corners of alternating $\text{V}^{\text{V}}\text{O}_4$ tetrahedra and MoO_6 octahedra. The remaining four V positions (2 V^{V} and 2 V^{IV}) are crystallographically disordered over nine potential sites of the lower hemisphere, where another $\mu_9\text{-Te}^{\text{IV}}\text{O}_3$ anion occupies the central cavity, with the lone pair of electrons pointing upwards. The assignment of formal charges on the metal ions was made on the basis of charge balance considerations for the entire compound, combined with bond valence sum (BVS) calculations,¹¹ elemental analysis, redox titrations and high resolution electrospray mass spectrometry.[†]

The V atoms in the VO_4 are coordinated by two $\mu_3\text{-O}^{2-}$ and one $\mu_2\text{-O}^{2-}$ moieties, with V–O bonds spanning the range 1.783(8)–1.810(8) and 1.682(10)–1.701(9) Å, respectively and one terminal oxo group with an average V=O distance of 1.597(9) Å. The MoO_6 alternating with the $\text{V}^{\text{V}}\text{O}_4$ tetrahedra complete their coordination environment with two terminal oxo groups in *cis*-positions, with Mo=O bonds (1.694(9)–1.724(8) Å), one $\mu_2\text{-O}^{2-}$, (2.062(8)–2.096(8) Å) and three $\mu_3\text{-O}^{2-}$ moieties in the range of 2.062(8)–2.250(8) Å. The Te atoms in the TeO_3 are coordinated with three $\mu_3\text{-O}^{2-}$ moieties, with an average Te–O bond length of 1.877(8) Å while the Te atom in TeO_4 is coordinated with four $\mu_2\text{-O}^{2-}$ in the range of 1.921(8) to 2.116(8) Å. Compound **3a** can be formulated as $[\text{Mo}^{\text{VI}}_{11}\text{V}^{\text{V}}_5\text{V}^{\text{IV}}_2\text{O}_{52}(\mu_9\text{-Te}^{\text{IV}}\text{O}_3)(\text{Mo}^{\text{VI}}_6\text{V}^{\text{V}}\text{O}_{22})]^{10-}$ which adopts a “Crowned”-Dawson structural motif and is isostructural to the sulfite-based $\{\text{M}_{25}\text{S}\}$ capsulae.⁹ Furthermore, the structural

similarities with compounds **1a** and **2a** become obvious since the lower part of their structures incorporates the same building block, $\{\text{Mo}^{\text{VI}}_8\text{V}^{\text{V}}_5\text{V}^{\text{IV}}_2\text{Te}^{\text{IV}}\text{O}_{48}\}$, see Fig. 3. In the case of **3a** there is a triad of edge-shared MoO_6 octahedra capping the $\{\text{Mo}^{\text{VI}}_8\text{V}^{\text{V}}_5\text{V}^{\text{IV}}_2\text{Te}^{\text{IV}}\text{O}_{48}\}$ unit, connected further to the “crown”-shaped, $\{\text{Mo}^{\text{VI}}_6\text{V}^{\text{V}}\text{O}_{22}\}$, formation while in the case of **1a** and **2a** the common building unit is capped by a $\{\text{Mo}^{\text{VI}}_4\text{V}^{\text{V}}_3\text{V}^{\text{IV}}_2\text{Te}^{\text{IV}}\text{O}_{33}\}$ and $\{\text{Mo}^{\text{VI}}_4\text{V}^{\text{V}}_3\text{V}^{\text{IV}}_2\text{Te}^{\text{IV}}\text{O}_{33}\}$ respectively. In a similar fashion to the $\{\text{M}_{18}\text{S}\}$ cluster⁹ in compounds **1a** and **2a**, the “crown” formation and the upper part of the capsule is crystallographically well resolved. The “crown”-shaped, $\{\text{Mo}^{\text{VI}}_6\text{V}^{\text{V}}\text{O}_{22}\}$ fragment is attached to the three $\text{Mo}^{\text{VI}}\text{O}_6$ centres located at the top of the ‘egg-shaped’ structure through six oxo-bridges. The metal sites in the lower hemisphere are crystallographically disordered over nine positions and the Mo, VO_4 and Te atoms can be assigned the oxidation states of VI, V and IV respectively (shown by BVS). Also, the V atoms in the VO_4 are coordinated by three $\mu_3\text{-O}^{2-}$ moieties, with V–O bonds spanning 1.730(6)–1.767(10) Å, and one terminal oxo group with V=O distances of the order of 1.628(11)–1.647(14) Å. The Mo atoms in the MoO_6 belonging to the upper hemisphere are coordinated by two terminal oxo groups in *cis*-positions, with Mo=O distances of 1.702(10)–1.731(12) Å, one $\mu_2\text{-O}^{2-}$, with Mo–O bond lengths between 1.882(10)–1.905(14) Å, and three $\mu_3\text{-O}^{2-}$ bridges, with Mo–O bond lengths of 1.988(10)–2.280(10) Å.[†]

During the course of this study, ESI-MS[†] has proved to be a valuable tool in our effort to discover the $\{\text{M}_{24}\text{Te}_3\}$ **1a** and $\{\text{M}_{24}\text{Te}_2\}$ **2a** clusters in solution. This was performed either directly in aqueous media or by precipitating solid from the various reaction mixtures *via* ion exchange with tetrabutyl ammonium (TBA) followed by using mass spectrometry in CH_3CN . In this study, the TBA salt of the $\{\text{M}_{24}\text{Te}_3\}$ cluster **1a**, dissolved in CH_3CN confirmed that the tellurite inorganic cage retains its integrity in solution (Fig. S1, ESI[†]), and peaks were seen that were assigned to the $\{\text{M}_{012}\text{V}_{12}\text{Te}_3\}$ species organized in two groups of envelopes (Fig. 4).

The higher intensity envelope comprises two overlapping species which can be formulated as $\{(\text{C}_{16}\text{H}_{36}\text{N})_3\text{K}_6\text{H}_3[\text{Mo}^{\text{VI}}_{12}\text{V}^{\text{V}}_4\text{V}^{\text{IV}}_8\text{O}_{69}\text{Te}(\text{TeO}_3)_2]\cdot(\text{H}_2\text{O})_8\}^{2-}$ at *m/z ca.* 2227.1 and $\{(\text{C}_{16}\text{H}_{36}\text{N})_3\text{K}_4\text{H}_3[\text{Mo}^{\text{VI}}_{12}\text{V}^{\text{V}}_6\text{V}^{\text{IV}}_6\text{O}_{69}\text{Te}(\text{TeO}_3)_2]\cdot(\text{H}_2\text{O})_{13}\}^{2-}$ at *m/z ca.* 2233.2, respectively. In the case of **2a** the studies

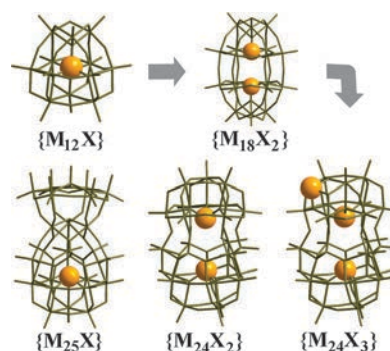


Fig. 3 A wire-stick representation of related HPOMs and their evolution from Keggin $\{\text{M}_{12}\text{X}\}$, Dawson $\{\text{M}_{18}\text{X}_2\}$ to the compounds described here, $\{\text{M}_{25}\text{X}\}$, $\{\text{M}_{24}\text{X}_2\}$ and $\{\text{M}_{24}\text{X}_3\}$. All the cages contain the same M_9X unit in the lower hemisphere and the heteroatom, X, is represented by an orange sphere.

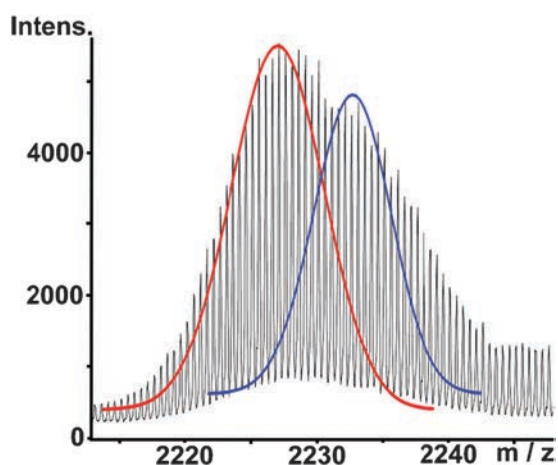


Fig. 4 Negative ion mass spectrum of **1a** in acetonitrile solution. Two envelopes can be seen centred at m/z ca. 2227.1 (with $8V^{IV}$) at m/z ca. 2233.2 (with $6V^{IV}$) respectively. Black line: experimental data, red/blue lines: profile lines of the simulated isotope patterns.

were performed in aqueous medium. As expected, the spectrum consists of a number of overlapping envelopes assigned to a range of species with varying levels of protonation and hydration (Fig. S3, ESI†). The main species observed give envelopes at m/z ca. 1776.7 and 2350.3 and are formulated as dimers of **2a** species, $\{K_{12}H_4[(Mo_{12}V_{12}O_{69}(TeO_3)_2)_2(H_2O)_{11}]^{4-}$ and $\{K_{11}H_6[(Mo_{12}V_{12}O_{69}(TeO_3)_2)_2(H_2O)_{10}]^{3-}$ respectively.

In conclusion, we have reported the discovery, syntheses and structural investigation of three novel mixed-metal, mixed-valence polyoxomolybdenum/vanadium-tellurite clusters $(NH_4)_9K[Mo^{VI}_{12}V^V_8V^{IV}_4Te^{IV}O_{69}(\mu_9-Te^{IV}O_3)_2]\cdot 27H_2O$ **1**, $K_{14}[Mo^{VI}_{12}V^V_8V^{IV}_4O_{69}(\mu_9-Te^{IV}O_3)_2]\cdot 27H_2O$ **2** and $K_{10}[Mo^{VI}_{11}V^V_5V^{IV}_2O_{52}(\mu_9-Te^{IV}O_3)(Mo^{VI}_6V^V O_{22})]\cdot 15H_2O$ **3** which belong to the ‘‘Crown’’-Dawson mixed-metal HPOM family templated by heteroanions from group *VIA*. The above compounds are the largest reported so far for mixed metal POMs which incorporate the pyramidal $Te^{IV}O_3$ anion. ESI-MS studies proved to be crucial not only for the discovery of the aforementioned compounds, but also to identify unambiguously the additional Te^{IV} atom which is incorporated in **1a**. Furthermore, we demonstrated the cooperative effect of the counterion along with the size of the hetero-ion which allowed the discovery and isolation of these novel POM-based compounds. We have already further expanded the mixed-metal polyoxometalate family, templated by non-conventional heteroanions, and an extensive heteroion size/structural correlation study has been performed and will be reported shortly.

Notes and references

† Crystal data for **1**: $(NH_4)_9K[Mo^{VI}_{12}V^V_8V^{IV}_4Te^{IV}O_{69}(TeO_3)_2]\cdot 27H_2O$: $H_{90}K_{10}Mo_{12}N_9O_{102}Te_3V_{12}$, $M_r = 4033.27$, monoclinic, space group $C2/c$, $a = 50.9979(13)$, $b = 13.6827(3)$, $c = 31.7935(8)$ Å, $\beta = 117.550(3)$, $V = 19669.5(8)$ Å³, $Z = 8$, $\rho_c = 2.724$ g cm⁻³, $\lambda(Cu-K\alpha) = 1.5418$ Å, $T = 150(2)$ K, 60 988 reflections measured, 15 368 independent reflections ($R_{int} = 0.0812$), $R_1(\text{final}) = 0.0712$, $wR_2 = 0.1938$, $GoF = 1.085$.

Crystal data for **2**: $K_{14}[Mo^{VI}_{12}V^V_8V^{IV}_4O_{69}(TeO_3)_2]\cdot 27H_2O$: $H_{54}K_{14}Mo_{12}O_{102}Te_2V_{12}$, $M_r = 4251.59$, monoclinic, space group $C2/m$, $a = 23.2791(6)$, $b = 13.3972(3)$, $c = 29.3216(8)$ Å, $\beta = 93.462(2)$, $V = 9127.8(5)$ Å³, $Z = 4$, $\rho_c = 3.094$ g cm⁻³, $\lambda(Cu-K\alpha) = 1.5418$ Å, $T = 150(2)$ K, 36 456 reflections measured, 9042 independent reflections ($R_{int} = 0.0746$), $R_1(\text{final}) = 0.0859$, $wR_2 = 0.2250$, $GoF = 1.055$.

Crystal data for **3**: $K_{10}[Mo^{VI}_{11}V^V_5V^{IV}_2O_{52}(TeO_3)(Mo^{VI}_6V^V O_{22})]\cdot 15H_2O$: $H_{30}K_{10}Mo_{17}O_{92}TeV_8$, $M_r = 4059.34$, orthorhombic, space group $Pnma$, $a = 15.3491(2)$, $b = 21.2977(2)$, $c = 25.9883(2)$ Å, $V = 8495.59(15)$ Å³, $Z = 4$, $\rho_c = 3.174$ g cm⁻³, $\lambda(Cu-K\alpha) = 1.5418$ Å, $T = 150(2)$ K, 23 939 reflections measured, 6889 independent reflections ($R_{int} = 0.0746$), $R_1(\text{final}) = 0.0678$, $wR_2 = 0.1907$, $GoF = 1.069$. Further details on the crystal structure investigation may be obtained from the ESI.†

- (a) D.-L. Long, E. Burkholder and L. Cronin, *Chem. Soc. Rev.*, 2007, **36**, 105; (b) D.-L. Long, R. Tsunashima and L. Cronin, *Angew. Chem., Int. Ed.*, 2010, **49**, 1736.
- (a) T. M. Anderson, X. Zhang, K. I. Hardcastle and C. L. Hill, *Inorg. Chem.*, 2002, **41**, 2477; (b) D.-L. Long, H. Abbas, P. Kögler and L. Cronin, *J. Am. Chem. Soc.*, 2004, **126**, 13880; (c) J. Zhang, D. Li, G. Liu, K. J. Glover and T. Liu, *J. Am. Chem. Soc.*, 2009, **131**, 15152; (d) H. N. Miras, G. J. T. Cooper, D.-L. Long, H. Bögge, A. Müller, C. Streeb and L. Cronin, *Science*, 2010, **327**, 72.
- (a) X. Fang and P. Kögler, *Angew. Chem., Int. Ed.*, 2008, **47**, 8123; (b) M. N. Sokolov, V. S. Korenev, N. V. Izarova, E. V. Peresypkina, C. Vicent and V. P. Fedin, *Inorg. Chem.*, 2009, **48**, 1805; (c) C. P. Pradeep, D.-L. Long, C. Streeb and L. Cronin, *J. Am. Chem. Soc.*, 2008, **130**, 14946; (d) S. G. Mitchell, C. Streeb, H. N. Miras, T. Boyd, D.-L. Long and L. Cronin, *Nat. Chem.*, 2010, **2**, 308; (e) X. Fang, P. Kögler, Y. Furukawa, M. Speldrich and M. Luban, *Angew. Chem., Int. Ed.*, 2011, **50**, 5212.
- (a) P. J. S. Richardt, J. M. White, P. A. Tregloan, A. M. Bond and A. G. Wedd, *Can. J. Chem.*, 2001, **79**, 613; (b) M. Pley and M. S. Wickleder, *Angew. Chem., Int. Ed.*, 2004, **43**, 4168.
- (a) K. Y. Matsumoto, M. Kato and Y. Sasaki, *Bull. Chem. Soc. Jpn.*, 1976, **49**, 106; (b) M. J. Manos, H. N. Miras, V. Tangoulis, J. D. Woolins, A. M. Z. Slawin and T. A. Kabanos, *Angew. Chem., Int. Ed.*, 2003, **42**, 425; (c) D.-L. Long, P. Kögler and L. Cronin, *Angew. Chem., Int. Ed.*, 2004, **43**, 1817; (d) H. N. Miras, R. G. Raptis, P. Baran, N. Laloti, M. P. Sigalas and T. A. Kabanos, *Chem.-Eur. J.*, 2005, **11**, 2295; (e) N. V. Izarova, M. H. Dickman, R. N. Biboum, B. Keita, L. Nadjo, V. Ramachandran, N. S. Dalal and U. Kortz, *Inorg. Chem.*, 2009, **48**, 7504; (f) J. Yan, D.-L. Long and L. Cronin, *Angew. Chem., Int. Ed.*, 2010, **49**, 4117; (g) H. N. Miras, J. D. Woolins, A. M. Slawin, R. G. Raptis, P. Baran and T. A. Kabanos, *Dalton Trans.*, 2003, 3668; (h) H. N. Miras, R. G. Raptis, P. Baran, N. Laloti, A. Harrison and T. A. Kabanos, *C. R. Chim.*, 2005, **8**, 957.
- (a) D.-L. Long, Y. F. Song, E. F. Wilson, P. Kögler, S. X. Guo, A. M. Bond, J. S. J. Hargreaves and L. Cronin, *Angew. Chem., Int. Ed.*, 2008, **47**, 4384; (b) J. Yan, D.-L. Long, E. F. Wilson and L. Cronin, *Angew. Chem., Int. Ed.*, 2009, **48**, 4376.
- (a) A. M. Todea, A. Merca, H. Bögge, T. Glaser, J. M. Pigga, M. L. K. Langston, T. Liu, R. Prozorov, M. Luban, C. Schroder, W. H. Casey and A. Müller, *Angew. Chem., Int. Ed.*, 2010, **122**, 514; (b) Q. Yin, J. M. Tan, C. Besson, Y. V. Geletii, D. G. Musaev, A. E. Kuznetsov, Z. Luo, K. I. Hardcastle and C. L. Hill, *Science*, 2010, **328**, 342.
- H. N. Miras, D. J. Stone, Eric J. L. McInnes, R. Raptis, P. Baran, G. I. Chilas, M. P. Sigalas, T. A. Kabanos and L. Cronin, *Chem. Commun.*, 2008, (39), 4703.
- H. N. Miras, M. N. C. Ochoa, D.-L. Long and L. Cronin, *Chem. Commun.*, 2010, **46**, 8148.
- M. T. Pope and A. Müller, *Angew. Chem., Int. Ed. Engl.*, 1991, **30**, 34.
- R. D. Shannon, *Acta Crystallogr., Sect. A: Cryst. Phys., Diffraction, Theor. Gen. Crystallogr.*, 1976, **32**, 751.